Development of Ni/HTA/Hβ alkane isomerization catalyst with improved selectivity for multi branched isoalkanes

Lijun Zhu

zhulijun@upc.edu.cn

China University of Petroleum, East China

Guosheng Huang

China University of Petroleum, East China

Shuo Liu

China University of Petroleum, East China

Xiaohui Jing

China University of Petroleum, East China

Junwei Yang

China University of Petroleum, East China

Daohong Xia

China University of Petroleum, East China

Research Article

Keywords: alkane isomerization, heteropoly acid, multi branched, isoalkanes

Posted Date: August 20th, 2025

DOI: https://doi.org/10.21203/rs.3.rs-7203210/v1

Additional Declarations: No competing interests reported.

Version of Record: A version of this preprint was published at Research on Chemical Intermediates on September 26th, 2025. See the published version at https://doi.org/10.1007/s11164-025-05742-x.

Abstract

Isoalkanes are ideal gasoline components, and the isomerization reaction of light alkanes is the most effective way to increase the octane number of gasoline. Non-precious metal/zeolite catalysts are the mainstream bifunctional catalysts for alkane isomerization reactions, but there are still challenges in achieving high octane number components - multi branched isoalkanes in isomerization reactions. In this article, Ni-heteropoly acid/zeolite alkane isomerization catalyst (Ni-HTA/Hβ) was prepared by impregnation method. Under optimized conditions, the conversion rate of n-hexane was 80.7%, the yield of isoalkanes was 79.8%, and the selectivity of isoalkanes was as high as 98.9%. In the product distribution, the Ni-HTA/Hβ catalyst can obtain more multi branched isoalkanes, namely 2,2-dimethylbutane and 2,3-dimethylbutane, with a total content of up to 19.2%, achieving the goal of further improving the yield of double branched alkanes in C_6 alkane isomerization products.

Highlights

(1) Ni-HTA/Hβ showed excellent hexane conversion rate and multi branched isoalkanes yield

(2) Coexistence of multiple types of acid distributions improved the isomerization of intermediates.

(3) The introduction of heteropolyacids can reduce cracking and increase the selectivity of isoalkane, especially multi-branched isoalkane.

1. Introduction

With the upgrading of environmental protection, clean gasoline products are developing towards high octane number, low sulfur, low olefins, low benzene, low aromatics, and low vapor pressure. Due to the activities of alkenes and aromatics in gasoline, the oil is prone to deterioration, or the concentration of pollutants in the combustion exhaust exceeds the standard, and it is easy to increase the sediment in the intake valve and combustion chamber. Therefore, the gasoline standards of many countries limit the content of aromatics and alkenes [1, 2]. But both aromatics and alkenes are high octane components (in Table S1), and the decrease in their content has a serious impact on the octane number of gasoline [3]. A consensus alternative solution is to increase the proportion of isoalkanes in the gasoline pool through the isomerization of C_5/C_6 alkanes, which can significantly increase the octane number of gasoline [4–6]. For example, after the isomerization of n-hexane to 2,2-dimethylbutane, the octane number increases by 67 units, while the isomerization of n-pentane to 2,2-dimethylpropane increases the octane number by 23 units. At present, C_5/C_6 alkane isomerization technology has become the mainstream gasoline upgrading technology for optimizing gasoline components.

At present, C_5/C_6 alkane isomerization catalysts widely used in industrial production include precious metal supported zeolite catalysts and aluminum chloride-based catalysts. Due to the fact that the active component is usually a precious metal such as Pt, it has the drawbacks of high cost and poor sulfur

tolerance [7–8]. For aluminum chloride-based catalysts, due to their abnormal sensitivity to moisture, they are prone to deactivation and require a large amount of catalyst consumption. Therefore, developing catalysts with high activity, good sulfur resistance, and low cost, especially those with excellent selectivity for multi branched isoalkanes, has become a very urgent technical demand for gasoline production enterprises.

Exploration and research on new catalysts have been ongoing, such as, Mih á lyi et al. prepared nickel loaded aluminum and/or boron containing BEA zeolites catalysts by recrystallization of magnetite variations, which were used for n-heptane isomerization [9]. The Ni/ZSM-5 + Al_2O_3 catalysts were prepared for transformation of n-hexane and the effect of metal support interactions in them were investigated further [10]. Zinc/HZSM-5 catalysts were prepared by impregnating zinc into HZSM-5 and their catalytic activity for n-pentane isomerization was studied [11]. Generally speaking, these non-precious metal catalysts are currently inexpensive, but the dispersibility is not as good as that of precious metal catalysts, leading to the need for further improvement in catalytic activity.

Heteropoly acid is a general term for condensed oxygen-containing acids produced by the condensation of different oxygen-containing acids. It is a type of oxygen-containing polyacid composed of heteroatoms (such as P, Si, Fe, Co, etc.) and polyatoms (such as Mo, W, V, Nb, Ta, etc.) in a certain structure, bridged through oxygen atom coordination. HPAs not only have acidity, but also have oxidation-reduction properties, thus possessing special catalytic activity. It is a green catalyst with both acid-base and oxidation-reduction properties

Due to the unique acidity, heteropoly acid has become an important modifier component in catalyst research for petroleum processing [10]. The strong acidity of HPAs makes them attractive candidates for addressing the current challenges of alkane isomerization [12–13]. However, current research mainly focuses on the preparation of supported heteropoly acid salt catalysts to improve the dispersion and low specific surface area of heteropoly acids, and has made certain progress [14, 15].

Essayem et al. [16] prepared a series of $H3PW_{12}O_{40}$ heteropoly acid catalysts using Pt-SiO_2 as a carrier, and their catalytic performance for n-hexane isomerization reaction were investigated. The experimental results showed that heteropoly acid have high catalytic activity for n-hexane isomerization reaction. Compared with Pt loaded dealuminated mordenite catalysts, although heteropoly acid catalysts have higher acid strength, they exhibit lower selectivity for dimethylbutane. Travers et al. [17] studied the catalytic performance of Pt/$CsxH_3$-x$PW_{12}O_{40}$ catalyst for the isomerization reaction of n-hexane. The conversion rate of n-hexane and the selectivity of isomeric alkanes were significantly improved, but the selectivity of multi branched isoalkanes did not significantly increase.

It is generally believed that in a bifunctional catalytic system, metal active centers play a role in catalyzing the hydrogenation of raw material molecules to produce alkenes, while acid sites catalyze the isomerization reaction of alkenes. Heteropoly acids, as a solid superacid, determine the unique overall

acidity and acid distribution characteristics of catalysts. The phosphotungstic acid (HPW) loaded on Ni/MCM-41 catalyst increases its strong acidity, thus strengthening the conversion pathways of hydrocracking and isomerization. After adding heteropoly acids, the strong acid density of the catalyst increases from 0.563 to 0.730 mmol/g [18]. HPWs exhibit better catalytic activity than MCM-41 in both hydrocracking and isomerization processes. Kozhevnikov [19] found that heteropoly acid had pure B-acid centers and exhibit higher catalytic activity than molecular sieves, but their thermal stability was generally poor, especially when reacting at temperatures ranging from 350 ^{o}C to 500 ^{o}C, the structure of the catalyst was destroyed.

Later, Kozhevnikov et al. [20] found that loading precious metals such as Pt and Pd onto HPAs through impregnation can improve the thermal stability and regeneration performance of the catalyst, while also significantly improving its catalytic performance.

Belandria et al. [21] loaded phosphotungstic acid onto mesoporous silica (with a loading amount of 30 wt.%) as a carrier, and further prepared Pt HWP/HMS catalyst by loading precious metal Pt or Pd onto the aforementioned carrier. The catalytic performance of Pt HWP/HMS catalyst for n-pentane isomerization was investigated at a reaction temperature of 200–400 ^{o}C, and the results showed that the catalyst had the best catalytic effect at a reaction temperature of 350 ^{o}C. Under the same reaction conditions, Pt HWP/HMS catalyst has higher catalytic activity for n-pentane isomerization than Pd HWP/HMS catalyst.

In the industrial application of isomerization process, the most concerned aspect is the selectivity of the catalyst, as low conversion in a single reaction can be overcome through a cyclic reaction that enters the reactor again or a series reaction. The high selectivity, especially for dimethylbutane with high octane number, determined the octane number of isomerization oil, which is particularly important for the industrial application of catalysts. At the same time, improving the selectivity of the high octane components can minimize the generation of cracking - i.e., C_4 and below components, which is also very important for improving liquid reception.

Travers et al. [22] successfully synthesized Pt $CsxH_3$-$xPW_{12}O_{40}$ catalyst by adjusting the stoichiometric ratios of $H_3PW_{12}O_{40}{\cdot}nH_2O$ and $Cs_3PW_{12}O_{40}$, and further investigated the catalytic performance of the catalyst for n-hexane isomerization. The results indicate that the catalytic performance of Pt-$CsxH_3$-$xPW_{12}O_{40}$ catalyst is similar to that of industrial molecular sieve catalyst, but the catalyst exhibits higher selectivity for double branched alkanes.

By adjusting the strength and proportion of acid centers, the selectivity of the catalyst can be improved. However, in general, the increase in acid ratio through changing preparation conditions or doping metal modification is limited. However, the introduction of heteropoly acids into the catalyst plays a decisive role in improving the strength and proportion of acids, thereby significantly improving the selectivity of multi branched isoalkanes. X. Yang et al. [23] reported on the noble metal catalyst Pt/MCM-41 grafted

with tungsten phosphate, where highly dispersed HPW produced approximately 143 of moderate strength μmol/g Bronsted acid sites. In the isomerization reaction of n-heptane, the conversion rate of n-heptane was 79.2%, and the isomerization selectivity was 100%. The ratio of multi branched isoalkanes to single branched isoalkanes ranged from 0.60 to 0.85. These results indicate that mesoporous catalysts exhibit unique shape selectivity in the skeletal isomerization of n-heptane.

The regulation of acidic sites can improve the selectivity of multi branched isoalkanes. For example, Fuente et al. prepared Pt/$H_3PW_{12}O_{40}$/SBA-15 trifunctional catalysts with high selectivity for hydroisomerization of n-heptane [24]. Lewis (L) and Brønsted (B) acid sites are present in the catalyst, and reduction treatment results in better dispersion of heteropoly acids and smaller Pt nanoparticles. The catalyst achieved 100% isomerization selectivity and 56.74% n-heptane conversion at 320 ° C. Among these products, the content of dibranched isoalkanes was greater than 50%, with 2, 2-dimethylpentane having the highest content. The author believes that the Pt nanocrystals, appropriate acidity, balanced B/L acid site ratio, and highly ordered large mesopores of the catalyst are the main reasons for high isomerization selectivity.

It is widely accepted that heteropoly acid type catalysts have high activity in alkane isomerization reactions, do not pollute the environment, and do not corrode equipment, making them a type of green and environmentally friendly catalyst [25]. By appropriately reducing the hydrogenation activity of metal active sites and promoting further isomerization reactions of intermediate products, thereby improving the selectivity for multi branched isoalkanes, it is considered an important way for industrial applications. At present, heteropoly acid catalysts mainly focus on improving the specific surface area by loading, and mainly use precious metals as metal active components. However, at present, heteropoly acid catalysts mainly focus on improving the specific surface area by loading, and mainly use precious metals as metal active components. There are few studies on the development of non-precious metal catalysts and improving the selectivity of multi branched isoalkanes.

The nickel phosphide supported β zeolite catalysts have been used in isomerization related research [26, 27], achieving good catalytic performance. In order to further improve the selectivity of multi branched isoalkanes, this article introduces ternary heteropoly acids into the catalyst system on the basis of strong acidic β-zeolite carriers, further adjusting the acid strength distribution of the catalyst. A novel alkane isomerization catalyst supported by nickel and heteropoly acids on β-zeolite was prepared and applied to catalyze C_5/C_6 alkane isomerization reaction. By improving the dispersion of metal active sites and utilizing heteropoly acids to improve the distribution of acid content and acidic sites, the hydrogenation activity and isomerization reaction activity are balanced, thereby increasing the selectivity of double branched isomeric alkanes and obtaining isomerized products with higher octane numbers.

2. Experiment

2.1 Materials

Sodium borohydride (A.R), ammonia-water (A.R) and nickel chloride hexahydrate ($NiCl_2{\cdot}6H_2O$, A. R) were purchased from Sinopharm Chemical Reagent Co., Ltd. Sodium molybdate ($Na_2MoO_4{\cdot}2H_2O$, AR), Sodium tungstate ($Na_2WO_4{\cdot}2H_2O{\cdot}2H_2O$, AR), Disodium phosphate ($Na_2HPO_4{\cdot}12H_2O$, AR) and sulfuric acid were supplied by Aladdin Reagent Co., Ltd. Hβ zeolites (Si/Al = 25) and n-hexane (A.R) were supplied by the catalyst plant of Nankai University and Xilong Chemical Co., Ltd, respectively. And commercial catalyst (Pt/H-mordenite) was provided by Dong ming Petrochemical Group and its platinum content was 0.4 wt. %.

2.2. Preparation of catalysts

Preparation of Ternary Heteropoly Acid (HTA)

50 mL of distilled water was placed in a 250 mL three necked flask equipped with a reflux condenser tube. The 3.630 g (0.015 mol) of $Na_2MoO_4 \cdot 2H_2O$ and 4.950 g (0.015 mol) of $Na_2WO_4 \cdot 2H_2O$ were added into the three-necked flask, stirring and heating until boiling. Then the 0.895 g (0.0025 mol) of $Na_2HPO_4 \cdot 12H_2O$ was added into the three-necked flask, stirred to dissolve and heated to boiling again.

After heating and refluxing for 30 minutes, 6 mol/L hydrochloric acid was added dropwise into the mixture, and the pH value of the reaction solution was adjusted to 1.0. After further refluxing for 5 hours, the three-necked flask was placed in a water bath and cooled to 60 ^{o}C.

Then the mixture was transferred to a separating funnel and about 15mL of ether was added before fully shaking. Then about 15mL of 1:1 sulfuric acid was dropped into the separating funnel, and oily substances appeared in the bottom of separating funnel. Then the oily substance was separated and placed in an evaporating dish. The 2–3 drops of distilled water were added. The ternary heteropoly acid-HTA as light-yellow green crystals precipitated after 1–2 days. According to the material calculationternary, the structure of the synthesized HTA is $H_3PMo_6W_6O_{40}$.

Preparation of Ni heteropoly acid/zeolite catalyst (Ni-HTA/Hβ)

By equal volume impregnation method, a certain amount of nickel nitrate and HTA were dissolved in a certain amount of deionized water, and then the Hβ zeolite was added into the solution and immersed for 24 hours. After drying at 110 ^{o}C for 4 hours, it was calcined at 400 ^{o}C for 4 h in a muffle furnace. Then the solid was crushed and sieved to obtain 20–80 mesh particles, which is the oxidized catalyst. After high-temperature reduction treatment in hydrogen of the oxidized catalyst, the Ni-HTA/Hβ with catalytic activity was finally obtained. In the process of preparing the catalyst, in addition to adding heteropoly acids, other processes are consistent with Ni-HTA/Hβ, resulting in the preparation of Ni/Hβ catalyst. The characterization methods and parameters of catalysts are included in the supporting information.

In order to investigate the effect of HTA content on catalyst performance, catalysts were prepared with HTA content of 10%, 20%, 30%, and 40% to the Hβ, and the other steps were the same as Ni-HTA/Hβ.

2.3 Catalyst performance evaluation process

The C_6 alkane isomerization performance evaluation of catalyst was carried out by using a high-pressure micro-reaction device. The reaction tube was a 550mm×8mm stainless steel tube. The reaction tube was filled with 4.0 g catalyst in the middle, and the two ends of the reaction tube were filled with quartz sand, so that the raw materials and hydrogen can be mixed evenly as far as possible. After checking the gas tightness, the reaction pressure was adjusted to the required conditions. i) Reduction: Before the reaction, the temperature was raised to 340 ^{o}C, so that the catalyst was reduced in hydrogen atmosphere for 4h. ii) Then, under the reaction conditions of reaction temperature, reaction pressure of 2.0 MPa, mass space velocity of 1.0 h^{-1} and molar ratio of hydrogen to oil of 4.0, the feed was started. 3) After the reaction was stable, the sample composition was analyzed by gas chromatograph.

3. Results and discussion

3.1. Characterization of catalyst

(1) BET

Nitrogen adsorption and desorption curves are consistent with the type IV isotherm. All the samples adsorbed nitrogen rapidly at low pressure, indicating that there were a large number of microporous structures in the samples, which were mainly generated by Hβ. In addition, in the P/Po of 0.4-1.0 pressure range, there is a hysteresis loop belonging to the H4 type in the curve, which indicates that mesoporous structures exist in all samples [28]. This is primarily attributed to the interparticle accumulation pores between heteropolyacids or heteropolyacids and zeolite. Compared with Hβ and Ni/Hβ, the fissure pore of Ni-HTA/Hβ was significantly reduced. Based on the nitrogen adsorption-desorption curve, the specific surface area, micropore volume and total pore volume were compared, and the results were listed in Table S2. The specific surface area and pore volume of the Hβ decreased after compounded with heteropoly acid, and decreased further after nickel loaded. This shows that as a supplement to acidity, heteropoly acid and metal-active nickel are distributed in the pore channels or mesopore of the zeolite. From the point of view of pore size distribution, the pore size distribution becomes more concentrated after the load is reduced. It shows that heteropoly acid and nickel enter into the pore and fully combine with zeolite. The full combination of Hβ, heteropoly acid and nickel on the microscopic level provided a guarantee for the catalytic activity.

(2) FT-IR

Infrared spectroscopy was used to characterize the functional groups inside the catalyst Ni-HTA/Hβ and compared with the infrared spectra of HTA and Hβ zeolites, and the results are shown in Fig. 3.

As can be seen from Fig. 3, the vibration peak of HTA are 1070.7 cm^{-1},981.8 cm^{-1},879.1 cm-1,784.7 cm^{-1},595.4 cm^{-1},518.6 cm^{-1}, respectively, which is consistent with the literature [29]. between 700–1100 cm^{-1}, the four characteristic peaks of the Kegan structure appeared, among which, 1050–1100 cm^{-1} is the expansion and contraction vibration wave number of P-O bond, and the 900–1000 cm^{-1} is the expansion

and contraction vibration wave number of M-O (M = Mo, W) bond. The 850–900 cm^{-1} is the telescopic vibration wave number of the M-O-M bridge (oxygen bridge of different groups of MO_6 octahedral bonds), and the 750–800 cm^{-1} is the telescopic vibration wave number of the M-O-M bridge (oxygen bridge of the same group of MO_6 octahedral bonds).

In addition, around 1620 cm^{-1} is the bending vibration number of H-O-H in water molecules [30]. It can be seen that the HTA are Keggin structures. On the other hand, Ni-HTA/Hβ and Hβ have similar infrared vibration peaks, indicating that the introduction of the active components HTA and nickel did not destroy the structure of Hβ zeolite.

Ni-HTA/Hβ has four characteristic peaks of Keggin structure, but the intensity of the four characteristic peaks of Keggin structure is weaker and the peak shape is broader compared to the FT-IR spectrum of HTA. It is accompanied by a weak blue shift in the wavenumber. It can be inferred that there is an interaction between the active component HTA and Hβ, which distorts the structure of HTA.

(3) Pyridine infrared

The pyridine adsorbed Fourier transformed infrared (Py-FTIR) spectroscopy

In order to further analyze the distribution of acidic sites on the surface of the catalyst, Py-FTIR spectroscopy was performed on the Ni-HTA/Hβ catalyst. As can be seen in Fig. 4, the sample at different temperatures has a hydrogen bond absorption band of pyridine around 1595 cm^{-1} [31]. The absorption peaks at approximately 1544 cm^{-1} and 1455 cm^{-1} can be attributed to pyridine adsorbed on the acidic sites of Brönsted (B) and Lewis (L), respectively [32, 33]. At the same time, a strong absorption peak appears at about 1450 cm^{-1}, which is attributed to the chemisorption of pyridine at the Lewis acid site [25, 34].

In addition, an absorption peak around 1575 cm^{-1} implies the presence of a weak Lewis acid site [32], [35], and the peak at 1620 cm^{-1} indicates the presence of strong acidic sites (SL). However, there is not a strong Lewis acid site at 1620 cm^{-1} of Hβ [26], indicating that the new acidic site formed after the compound of heteropoly acid and nickel with the support. It is believed that the number of strong Lewis acid sites is related to Ni and heteropoly acid, while the Brønsted acid sites are generated by the support, and the strong Lewis acid site at 1620 cm^{-1} plays an important role in promoting the performance of the alkane isomerization reaction.

The effect of temperature on the acidic position of the surface was further investigated. From the experimental results, it can be found that the overall peak intensity decreases with the increase of temperature. The absorption band of hydrogen bond pyridine located at 1595 cm^{-1} disappeared, due to the desorption of the pyridine molecule. All the other peaks have not disappeared. This shows that under the conditions of catalyst preparation and reaction temperature, the acidic and basic sites of the catalyst

will not be destroyed, and the acidic site of the catalyst can effectively play the role of isomerization reaction.

(4) H_2-TPR

The precursor of Ni-HTA/Hβ obtained after roasting was analyzed by H_2-TPR to investigate the appropriate reduction temperature of the catalyst. The experimental results are shown in Fig. 5.

As can be seen from Fig. 5, there is a significant reduction peak as the temperature gradually increases from 300 ^{o}C to 700 ^{o}C for 3 samples. When the temperature is higher than 300°C, the TPR signal value increases slowly, which is mainly due to the reduction of NiO and HTA on the surface of the carrier to metal Ni and new species in the hydrogen atmosphere. When the temperature is higher than 400°C, the TPR curve increases rapidly and significantly, which indicates that the active components on the surface are reduced by hydrogen, and a large amount of hydrogen is consumed. The above results show that nickel in the oxidized state can be reduced at the reaction temperature, and the nickel is mainly in the form of reduced species [36]. At the same time, the structure of the HTA is $H_3PMo_6W_6O_{40}$, in this hydrogen atmosphere, some HTA structures are disrupted, releasing P, Mo, and W atoms. These atoms may interact with the carrier or Ni to produce new species.

Above 500 ^{o}C, the three curves appear significant differences. The author believes that this is due to the presence of a large amount of heteropolyacid on Ni-HTA/Hβ, which is reduced to produce hydrogen gas consumption under high temperature conditions. However, the reduction of Ni/Hβ mainly comes from nickel, but the loaded amount of nickel is small, so the reduction peak is relatively low.

(5) NH_3-TPD

Comparative analysis by NH_3-TPD was conducted on HTA-Ni/Hβ, Ni/Hβ, and $NiNO_3$, as shown in Fig. 6. As can be seen from the Fig. 6, firstly, nickel nitrate has no acidity, so no desorption peak was detected. Compared to Ni/Hβ, due to the introduction of heteropolyacid into the catalyst, the Ni-HTA/Hβ has three ammonia desorption peaks, and their maximum values are around 270°C, 430°C and 550°C, respectively, indicating that there are three different types of acidic sites on the surface of the catalyst. The ammonia desorption temperature in the NH_3-TPD spectrum is related to the strength of the acidic site on the catalyst surface. When the catalyst peaks in the range of ammonia desorption temperature below 300°C, it indicates that the catalyst has a weak acid position, when the ammonia desorption temperature peaks in the range of 300–500°C, it indicates that the catalyst has a moderately strong acid position, and when the desorption temperature peaks in the range of 500°C, it indicates that the catalyst has a strong acid or super acid position [37, 38]. Therefore, the Ni-HTA/Hβ catalyst has a relatively large number of weak acid centers, some moderately strong acid centers, and relatively few strong acid centers.

Comparing several samples, it was found that the strong acids were mainly derived from nickel-loaded zeolites, while the introduction of heteropoly acid significantly increased the number of weakly acidic

sites [39]. The weakening of the acid site after loading the metal nickel is due to the fact that some of the metal occupies the acid site, which reduces the strength of the acid site through the action of an electron donor [40].

In conclusion, the three types of Ni-HTA/Hβ are abundant in acidic sites, with weakly acidic sites, moderately strong acidic sites, and strongly acidic sites. The coexistence of multiple types of acidic sites may be an important reason for the high catalytic activity. This is because in the alkane reaction process, the carbocation intermediate can fully isomerize at the abundant acidic site, providing sufficient reaction sites to ensure the conversion rate and selectivity of multiple branched alkanes.

(6) Morphological characteristics

The morphological features of the as-prepared samples were evaluated by both SEM and TEM imaging. The Fig. 7 and Fig. 8 illustrated the morphologies of the catalyst.

As can be seen from the SEM diagram, the catalyst looks uniform. On the surface, there is no obvious gathering of hybrid acid and nickel salt. It can be seen from the SEM-MAPPING diagram that the distribution of Ni, P, W, Mo, O element on the surface of the particles is evenly distributed, indicating that the HTA and nickel are evenly scattered on the carrier. The experimental results are consistent with the XRD results. Uniformly distributed appearance of active components on the surface of the carrier have an important role in the performance of catalytic performance. The experimental results consistently reflect the distribution of active components on the catalyst.

The NiP nanoparticles are usually spherical or chain shaped and interconnected, and their average diameter is about 100 nm [26]. By statistically analyzing the particle size in TEM images, the particle size distribution ranges from 1.0 to 3.1 nm, with an average size of 1.74 nm. The nickel nanoparticles of Ni-HTA/Hβ, the aggregation of Ni is effectively inhibited. Moreover, after the introduction of heteropoly acid, it is evident that nickel nanoparticles are more evenly distributed on the carrier. In Fig. 7B, the dispersed black particles are nickel particles, which are the active sites for hydrogenation and dehydrogenation catalysis.

The particle size of most nickel particles is around 1–3 nm with uniform distribution. Nickel has been well dispersed. This may be because heteropoly acid is rich in phosphorus atoms, which can prevent the aggregation of nickel. [41]

(7) XPS

In order to verify the combination form and chemical composition of nickel and heteropoly acid of the catalyst on the support, the samples were further studied by high resolution XPS spectrum analysis, as shown in Fig. 9, meanwhile Table S3 indicates the atomic concentration for narrow scan. The XPS survey spectrum (Fig. 9a) confirms the presence of C, O, P, Si, Mo, Ni and W elements, further indicating that nickel and heteropoly acid had been successfully introduced and loaded onto β zeolite.

Correspondingly, in the case of O 1s XPS (Fig. 9b), the spectrum of O 1s could be fitted by four peaks at binding energies of 531.2, 532.6, and 533.3 eV, which are ascribed to the W-O-W, P-O, and C-OH, respectively [42, 43], the peak at around 531.9 eV was originated from Si-O bonds [44]. This confirmed the structural integrity of zeolite and heteropoly acid carriers [43].

The binding energy of Ni^{2+} is 862.5 and 856.4, corresponding to Ni $2p_{1/2}$ and Ni $2p_{3/2}$, respectively, and high-binding energy belongs to Ni^{2+} species [45]. In general, Ni($2p_{3/2}$) binding energy is generally in the range of 855.6-856.6 eV. For example, according to literature, the $2p_{3/2}$ binding energy of Ni (II) is generally 854.6eV or 855.1eV [46, 47]. Compared with reported nickel ions, the binding energy 856.4 of Ni-HTA/Hβ (Fig. 9c) is shifted towards higher binding energy, which makes Ni^{2+} exhibit stronger electron deficiency. This may be due to the influence of heteropolyacids on nickel. The enhanced electron deficiency is more favorable for nickel to activate hydrogen molecules, so the overall isomerization catalytic activity of Ni-HTA/Hβ is enhanced.

The high-resolution XPS spectrum of W4f (Fig. 9d) presented four peaks at 35.8 eV and 34.9 eV，37.0 eV and 37.9 eV [48]. The binding energies of $W4f_{7/2}$ and $W_{4f5/2}$ are 35.8 and 37.9eV respectively (area ratio 4:3). The position and shape of these peaks represent the W (VI) oxidation state [49]. In addition, at the lower binding energies $W4f_{7/2}$=34.9 eV and $W4f_{5/2}$=37.0 eV, there are two distinct peaks (area ratio 4:3), which are related to the reduced W (V) ions on the catalyst surface, indicating that during the preparation of the catalyst, these heteropoly acids are partially reduced by hydrogen to produce low-valent tungsten [50]. This chemical binding energy characteristic of tungsten can be attributed to the tungsten-oxygen octahedron structure in Keggin unit [51].

The high -resolution spectrum of Mo 3d is shown in Fig. 9e. Due to the division of spin-orbit, the peak can be divided into Mo $3d_{5/2}$ and Mo $3d_{3/2}$. The peaks at 232.6 eV and 235.3 eV belong to Mo^{6+}, and the peaks at 231.4 eV and 234.3 eV belong to Mo^{5+} [52, 53]. Mo^{5+} should be generated by the reduction of the heteropoly acid, which indicates the formation of heteropoly acid. Moreover, the peaks of 229.8 eV and 233.3 eV come from the contribution of phosphorum molybdenum. The source of high -valent molybdenum may be caused by air oxidation during the preparation process. This result is consistent with the high -resolution O1S spectrum [26].

For high -resolution spectrum of P2p (in Fig. 9f), it can only be observed one peak at 133.9 eV, because the content of phosphorus is very low. The binding energy of 133.9 eV can be attributed to the oxidation state of phosphorus. Generally speaking, the binding energy of phosphotungstic acid is 134.5 eV [54]. The binding energy is closer to the binding energy (133.9 eV) of NiP [26]. Compared with phosphotungstic acid, the binding energy shifted to a lower field, which indicated that, under the preparation conditions, the nickel acted with phosphorus in heteropoly acid. This increases the exposure of active sites, improves the high-temperature stability of nickel species, and has a significant inhibitory effect on the high-temperature deactivation of catalysts.

On the other hand, from the atomic distribution on the catalyst surface in Table S3, the mass fractions of W, P, and Mo are 7.4%, 0.2%, and 3.6%, respectively. According to the valence state coordination of oxygen atoms, the mass fraction of ternary heteropoly acid is calculated to be about 14%, which is lower than the amount of heteropoly acid added at 20%. This may be due to the preferential entry of heteropoly acids into the pores after dissolving in water during the loading process, while the heteropoly acid located on the surface migrate, and some heteropoly acid enter the pores of the zeolite. In addition, thermal decomposition occurred during the roasting process, resulting in the loss of phosphorus element, and the content decreased to 0.2%, which was lower than the added amount (0.8%). The proportion of Ni atoms obtained from the test is 2.0%, which is consistent with the amount added, indicating that the nickel substance has not been lost.

3.2 Isomerization reaction performance of Ni-HTA/Hβ for n-hexane

A series of Ni-HTA/Hβ catalysts were prepared by equal-volume impregnation method according to different heteropoly acid loads. The Ni load content was 2%, and the HTA load content was 0, 10%, 20%, 30% and 40%, respectively. The Ni-HTA/Hβ catalyst was investigated by calcination at 400 ^{o}C for 4h in Muffle furnace and reduction at 400 ^{o}C for 4h, as shown in Fig. 10.

As can be seen from Fig. 10 (a), with the increase of HTA load content of heteropoly acid, the n-hexane conversion and isoalkanes yield gradually decreased, while the selectivity of isoalkanes showed a trend of first increasing and then decreasing. From the analysis of the mechanism of alkane isomerization reaction, the metal center of the catalyst used for mainly the hydrogenation/dehydrogenation of alkane and alkene, while the acidic center used for mainly the skeleton isomerization and cracking reaction. Therefore, the matching between the metal center and the acid site of the catalyst is the key factor affecting the catalytic performance of n-hexane isomerization reaction. When the HTA loading of heteropoly acid was 0 and 10%, the conversion of n-hexane was the highest, but the selectivity was low. When the loading amount of heteropolyacid was low,, the dehydrogenation reaction ability is relatively stronger, and a large amount of n-hexane dehydrogenates to produce olefins on the metal center, so the conversion of n-hexane was high. Excessive strong acid sites leaded to significant cracking reactions, so the high content of C_5 and C_{4-2} alkanes was detected. With the increase of HTA, the number and distribution of acidic sites underwent changes. When the loaded HTA was 20%, the metal activity on the catalyst surface matched with the acid activity. Although the conversion rate was not high, the selectivity was the highest, reaching 98.3%. When the HTA load was higher than 20%, the acid centers were sufficient, but the metal centers were obviously insufficient, resulting in the reduction of catalytic activity, the conversion rate and the yield.

Figure 10 (b) showed the change of total isohexane content, total C_5 alkane content and total ≤ C_4 alkane content with the change of HTA load content. With the increase of HTA load content, the total content of C_5 alkane and C_{4-2} alkane decreased first and then increased, while the total content of isohexane increased first and then decreased gradually with the increase of HTA load content. When the HTA load

was 20%, the total isohexane content reached the highest content (76.7%), while the total C_5 alkane content and the total ≤ C_4 alkane content reached the lowest (1.1% and 1.7%, respectively). In this case, the matching degree between the metal center and the acid center of the catalyst was the best, and the side reactions such as cracking reaction were less. The catalyst showed excellent catalytic isomerization performance.

It can be seen from Fig. 10 (c) that with the increase of HTA load of heteropoly acid, the contents of four hexane isomers showed the same change trend, and their contents increased first and then decreased with the increase of HTA load. The contents of 2-methylpentane, 3-methylpentane and 2, 3-dimethylbutane were similar to the contents of isohexane. When the heteropoly acid load was 20%, the contents of these three hexane isomers reached the maximum value. It is obvious that the optimal HTA load content for Ni-HTA/Hβ catalyst is 20%, the conversion rate of n-hexane is 79.5%, the yield of isoalkanes is 78.1%, and the selectivity of isoalkanes is 98.3%. Among them, the total content of dimethyl butane also reached the highest, which was 17.6%.

Therefore, this indicates that the introduction of heteropolyacids can regulate acid distribution. The medium-strong acidity of the catalyst is more favorable for the isomerization reaction of intermediates, while strong acidity tends to lead to the cracking reaction of carbocations. The medium-strong acidity provides active sites for the cracking of carbocations. Therefore, the introduction of heteropolyacids can reduce cracking and increase the selectivity of isoalkane, especially multi-branched isoalkane.

Figure 11 showed the reaction mechanism of dehydrogenation-isomerization-hydrogenation of n-alkanes on Ni-HTA/Hβ to prepare multi branched alkanes, with the isomerization reaction mechanism of carboncation in central illustration. The n-alkane first undergo dehydrogenation at the Ni active site to obtain n-alkene, which then undergo a proton transformation at the acid center to become a carboncation. The carboncation undergo isomerization reactions to generate multi branched carboncation. Multiple methyl transfer reactions and electron transfer reactions occur during the isomerization process of carbocation. This also indicates that in order to improve the selectivity of multi branched alkanes, sufficient reaction time and space must be provided for carbocations. Next, the isomeric carbocation loses one proton to generate isomeric olefin. Finally, the alkene is hydrogenated at the Ni active site to generate multi branched isoalkanes. From the perspective of reaction mechanism, the hydrogenation activity and isomerization activity must be finely matched to achieve high selectivity. This is also the fundamental reason for the excellent performance of the Ni-HTA/Hβ catalyst.

3.3 Investigation of long-term operation performance of catalysts

From Fig. 11(d, e, f), it can be seen that the conversion rate and selectivity of the catalyst remain stable within 60 hours, and the product distribution remains stable during the investigation time, indicating that the catalytic activity of Ni-HTA/Hβ has reached a stable state. The catalyst has excellent stability, and after isomerization of n-hexane, a large number of isomeric alkanes are generated, especially double

branched alkanes reaching 19.2%, which plays an important role in providing octane numbers for light alkanes. This catalyst is suitable for further industrial application testing.

In the products of isomerization reaction, there are isobutane, isopentane, and four isomers of hexane (including 2-methylpentane, 3-methylpentane, 2,3-dimethylbutane, and 2,2-dimethylbutane). In the product distribution, 2-methylpentane and 3-methylpentane have lower octane numbers, with research octane numbers (RON) of 74.4 and 75.5, respectively. However, 2,3-dimethylbutane and 2,2-dimethylbutane have higher octane numbers, with RON of 103.5 and 91.8, respectively. Therefore, increasing the content of dimethyl butane in the product of n-hexane isomerization reaction plays a very important role in improving the octane number of gasoline.

Table 1
Comparison of catalytic performance of various catalysts for n-hexane isomerization reaction

item/%	Ni-HTA/Hβ	NiB/Hβ[27]	NiP/Hβ[26]	commercial sample
Conversion rate	80.7	75	77.8	86.4
isoalkanes selectivity	98.9	80.1	93.7	88.1
isoalkanes yield	79.8	65.2	76.2	76.2
multi branched isomerizations	19.2	14.2	18.9	16.6

In order to compare the performance of catalysts, several common catalysts and commercial catalysts were evaluated under the same laboratory conditions, and the data obtained are shown in Table 1. According to Table 1, in terms of conversion rate, NiB/Hβ, and commercial catalysts (Pt/zeolite) have higher conversion rates for n-hexane, about 4–6 percentage points higher than Ni-HTA/Hβ catalysts. However, in terms of the selectivity of isomerizations, the Ni-HTA/Hβ has the highest selectivity of isomerization, reaching up to 98.9%. In addition, the proportion of multi branched isoalkanes in the product of Ni-HTA/Hβ catalyst is the highest, much higher than other catalysts, which can significantly increase the octane numbers. This is because the introduction of heteropoly acid into the catalyst provides the abundant acidic sites of weak acid, medium strong acid, and strong acid. The coexistence of multiple types of acidic sites improves the isomerization activity of Ni-HTA/Hβ, which has a positive effect on the selectivity of multi branched isomerizations. On the other hand, heteropoly acid, under the influence of heteropoly acidity, high-temperature aggregation of the nickel in Ni-HTA/Hβ is reduced, which provides more hydrogenation and dehydrogenation active sites for catalytic reactions. Therefore, this can promote the intermediate to undergo multiple isomerization reactions more easily, thereby obtaining multi branched isoalkanes.

4. Conclusion

In the process of alkane isomerization, improving the conversion rate and selectivity of catalysts is the most important research goal of this technology. Improving the selectivity of multi branched isoalkanes

plays a very important role in increasing the octane number of the gasoline. Under optimized reaction conditions, the Ni-HTA/Hβ catalyst exhibitd excellent isomerization performance. The conversion rate of n-hexane was 77.9%, the yield of isoalkanes was 77.4%, and the selectivity of isoalkanes was as high as 99.4%. In the product distribution, more double branched isomers were obtained, namely 2,2-dimethylbutane and 2,3-dimethylbutane, with a total content of 19.2wt%.

The characterization of the catalyst proved that the nickel active component and HTA were uniformly dispersed on the carrier, at the same time, the acid distribution was optimized by heteropolyacid. The medium-strong acidity site was more favorable for the isomerization reaction of intermediates. The introduction of heteropolyacids can reduce cracking and increase the selectivity of isoalkane, especially multi-branched isoalkane.

Declarations

Declaration of competing interest

The authors declare that they have no known competing financial interests or personal relationships that could have appeared to influence the work reported in this paper.

Acknowledgements

This work was financially supported by the Natural Science Foundation of Shandong Province (ZR2019MB057), the Fundamental Research Funds for the Central Universities (18CX02118A) and State Key Laboratory of Heavy Oil (SKLHOP202101010).

References

1. Song J.H, Zhang T.F, Xing M. J, et, al. Si-OH defect healing treatments of ZSM-22 zeolites for enhanced performance and alcohol resistance in n-alkanes hydroisomerization. Fuel 2025; 382:133683.
2. Setiabudi H.D, Jalil A.A, Triwahyono S, et al. Ir/Pt-HZSM5 for n-pentane isomerization: effect of Si/Al ratio and reaction optimization by response surface methodology. Chemical Engineering Journal 2013; 217: 300-309
3. Meyer C, Hager V, Schwieger W, Wasserscheid P. Enhanced activity and selectivity in n-octane isomerization using a bifunctional SCILL catalyst. Journal of Catalysis 2012; 292: 157-165.
4. Maciej S, Zbigniew K. C_6-alkane conversion over γ-alumina supported palladium and platinum catalysts. Chemical Engineering Journal 2002; 90: 89-96.
5. Zhang R, Ju Y.N, Wu P, et, al. Efficiently reducing olefin content of FCC gasoline over ZSM-5 zeolite based catalyst via hydro-upgrading. Catalysis Today 2022; 405: 57-65.
6. Wu X.R, Lei X.Q, Wang S.D, et, al. Tuning the acidity and pore structures of NiP based bifunctional catalyst for efficient n-hexane isomerization. Fuel 2022; 324.

7. Essayem N, Taârit Y.B, Feche C, et al. Comparative study of n-pentane isomerization over solid acid catalysts, heteropolyacid, sulfated zirconia, and mordenite: dependence on hydrogen and platinum addition. Journal of Catalysis 2003; 219: 97-106.
8. Santiesteban J.G, Calabro D.C, Chang C.D, et al. The role of platinum in hexane isomerization over Pt/FeOy/WOx/ZrO2. Journal of Catalysis 2001; 202: 25-33.
9. Mihályi R.M, Lónyi F, Beyer H.K, Szegedi Á, Kollár M, et al. n-Heptane hydroconversion over nickel-loaded aluminum- and/or boron-containing BEA zeolites prepared by recrystallization of magadiite varieties. Journal of Molecular Catalysis A: Chem 2013; 367:77-88.
10. Masalska A, Grzechowiak J.R, Jaroszewska K. Effect of metal-support interactions in Ni/ZSM-5 + Al_2O_3 catalysts on the transformation of n-alkanes. Topics in Catalysis 2013; 56: 981-994.
11. Triwahyono S, Jalil A.A, Mukti R.R, et al. Hydrogen spillover behavior of Zn/HZSM-5 showing catalytically active protonic acid sites in the isomerization of n-pentane. Applied Catalysis A: Gen 2011; 407: 91-99.
12. Teresa P, Veronique D, Frederic L. Isomerization of n-hexane on heteropolyacids supported on SBA-15. 1. Monofunctional impregnated catalysts. Applied Catalysis A: General 2014;483: 103-109.
13. Firouzjaee, Mahjoobeh Hajitabar, Taghizadeh, Majid. n-Butane Isomerization over 0.5 Pt/HPA/MCM-41 Catalyst: Optimization Study Using Central Composite Design. Chemical Engineering & Technology 2024; 6: 887-896.
14. Sun J.H, Li Y, Mu C, et al. Supported heteropolyacids catalysts for the selective hydrocracking and isomerization of n-C16 to produce jet fuel. Applied Catalysis A: General 2020; 598: 117556.
15. Yang W, Billy J, Taarit Y B, et al. $H_3PW_{12}O_{40}$ supported on Cs modified mesoporous silica: catalytic activity in n -butane isomerisation and in situ FTIR study. Catalysis Today 2002; 73: 153-165.
16. Essayem N, Taarit Y B, Gayraud P Y, et al. Heteropolyacid catalysts for hydro- isomerization of n-hexane: effects of alkali salt modification. Journal of Catalysis 2001; 204:157-162.
17. Travers C, Essayem N, Delage M, Quelen S. Heteropolyanions based catalysts for alkanes isomerization. Catalysis Today 2001; 65: 355-361.
18. Zhang Z, Cheng J, Zhu Y.X, et al. Jet fuel range hydrocarbons production through competitive pathways of hydrocracking and isomerization over HPW-Ni/MCM-41 catalyst. Fuel 2020; 269: 117465.
19. Kozhevnikov I.V. Catalysis by heteropoly acids and multicomponent polyoxometalates in liquid-phase reactions. Chemical Reviews 1998; 98: 171-198.
20. Kozhevnikov I. V. Sustainable heterogeneous acid catalysis by heteropoly acids. Journal of Molecular Catalysis A: Chemical 2010; 41: 86-92.
21. Belandria L, Marín A. N, Garcia E, Sosa E, et al. Catalytic activity of Pt and Pd catalysts supported on HWP/HMS in the selective hydroisomerization of n-pentane. Effect of reaction temperature. Catalysis Today 2011;172: 2-7.

22. Travers C, Essayem N, Delage M, Quelen S. Heteropolyanions based catalysts for alkanes isomerization. Catalysis Today 2001; 65: 355-361.
23. Yang X.K, Wang J.A, Chen L.F, et al. Heteropolyacid grafted Pt/Si-MCM-41 catalyst for C_7 skeletal isomerization. Catalysis Communications 2012; 28: 202-206.
24. Fuente N.D.L, Wang J.A, Chen L.F, et, al. Skeletal isomerization of n-heptane with highly selective Pt/$H_3PW_{12}O_{40}$/ SBA-15 trifunctional catalysts. Catalysis Communications 2017; 102: 93-97.
25. Marcelly M. B. Silva, Camila G. Vieira, Kelly A. da Silva Rocha. Heteropoly acid-catalyzedβ-caryophyllene chemical transformations: Synthesis route of value-added commercial products from components found in biorenewable resources. Molecular Catalysis 2023; 547:113302.
26. Chen J.S, Duan Z.B, Song Z.Y, et, al. Relationship between surface property and catalytic application of amorphous NiP/Hβ catalyst for n-hexane isomerization. Applied Surface Science 2017;425: 448-460.
27. Chen J.S, Cai T.T, Jing X.H, et al. Surface chemistry and catalytic performance of amorphous NiB/Hβ catalyst for n-hexane isomerization. Applied Surface Science 2016; 390: 157-166.
28. Hung M.J, Lin Y.W, Lin W.T, et al. Functionalization of mesoporous Al-MCM-41 for indoor humidity control as building humidity conditioning material. Journal of Molecular Structure 2024; 1299:137024.
29. Salles L, Piquemal J.Y, Thouvenot R, et al.Catalytic epoxi-dation by heteropolyoxoperoxo complexes:from novel pre-cursors or catalysts to a mechanistic approach. Journal of Molecular Catalysis A: Chemical 1997;117: 375-387.
30. Yong T K, Jung K D, Park E D. Gas-phase dehydration of glycerol over ZSM-5 catalysts. Microporous & Mesoporous Materials 2010; 131: 28-36.
31. Chakraborty B, Viswanathan B. Surface acidity of MCM-41 by in situ IR studies of pyridine adsorption. Catalysis Today 1999;49: 253-260.
32. Lin G, Bao X, Yu F, Gang S, Bai D. Impact of cationic surfactantchain length during SAPO-11 molecular sieve synthesis on structure acidity,and n-octane isomerization to di-methyl hexanes. Journal of Catalysis 2012;294:161-170.
33. Chen L.F, Zhou X.L, Norena L.E, et al. Comparative studies of Zr-based MCM-41 andMCM-48 mesoporous molecular sieves: synthesis and physicochemical properties . Applied Surface Science 2006; 253: 2443-2451.
34. Casagrande M, Moretti E, Storaro L, et al. Synthesis and structural characterization of MSU-type silica-tin molecular sieves: post-synthesis grafting of tin chlorides. Microporous and Mesoporous Materials 2006; 91: 261-267.
35. Ye Y.F, Cui Y.Y, Yang L, et al. B-containing ionic liquid modified SBA-15 for CO_2-epoxide coupling reaction metal-free catalysis. Journal of Colloid and Interface Science 2025; 680: 596-607.
36. Xie K.Y, Jiang B.S, Wang Z, et al. Study on the performance and sulfur tolerance mechanism of Pd/beta zeolite in catalytic combustion of toluene. Journal of Materials Research and Technology

2023; 25:4543-4553.

37. Zou C, Meng J.P, Zhao J.S, et, al.Enhanced hydroisomerization performance over highly mesoporous ZSM-48 zeolites constructed by organosilane surfactant. Molecular Catalysis 2024; 561:114160.
38. David P.S, Guillermo C, Juan A.B, et al. Characterization of adsorptive and hydrophobic properties of silicalite-1, ZSM-5, TS-1 and Beta zeolites by TPD techniques. Separation and Purification Technology 2007; 54: 1-9.
39. Camiloti A.M, Jahn S.L, Velasco N.D, et al. Acidity of Beta zeolite determined by TPD of ammonia and ethylbenzene disproportionation. Applied Catalysis A: General 1999; 182: 107-113.
40. Siva S.R.P, Susanne M, Anders R, Rasmus F. Heteropoly acid promoted Cu and Fe catalysts for the selective catalytic reduction of NO with ammonia. Catalysis Today 2010;176: 292-297
41. Yang X.H, Qiao J.G, Deng J.Y, et al. Role of H-beta zeolite on photocatalytic pollutant degradation and H_2 production enhancement of g-C_3N_4/H-Beta composite. Journal of Environmental Chemical Engineering 2023; 11:110828.
42. H. Wang, C. Wang, Y. Yang, et al. H3PW12O40/mpg-C_3N_4 as an efficient and reusable bifunctional catalyst in one-pot oxidation-Knoevenagel condensation tandem reaction. Catal. Sci. Technol. 7 (2017). 405-417.
43. Zeng X.Y, Xiao X.Y, Chen J.Y, Wang H.L. Electron-hole interactions in choline-phosphotungstic acid boosting molecular oxygen activation for fuel desulfurization. Applied Catalysis B: Environmental 2019; 248: 573-586.
44. Zhu Z.G, Ma H.K, Xu H, et al. Oxidative desulfurization of model oil over Ta-Beta zeolite synthesized via structural reconstruction. Journal of Hazardous Materials 2020; 393: 122458.
45. Song H, Wang J, Wang Z.D, et al. Effect of titanium content on dibenzothiophene HDS performance over Ni2P/Ti-MCM-41 catalyst. Journal of Catalysis 2014; 311: 257-265.
46. Nathan R, Jerome E, Nathalie E, et, al. An XPS and TEM study of the composition and structure of native oxides on the inner surface of as-received Ni base alloy steam generator tubes. Applied Surface Science 2024; 654:159514.
47. Na Z.C, Pan L.Y, Yao H.D, et al. Preparation of core-shell Ni/CeO_2@Al_2O_3 catalyst for selective hydrogenation of acetylene. Catalysis Communications 2024; 187: 106860.
48. Li J.P, Chen W.L, Chen L, et al. Strategy to Obtain Long-Term Stable Heteropoly Blues for Photosensitive Property Investigations. Advanced Optical Materials 2018; 6:14.
49. Zeng X.G, Xiao X.Y, Chen J.Y, et al. Electron-hole interactions in choline-phosphotungstic acid boosting molecular oxygen activation for fuel desulfurization. Applied Catalysis B: Environmental 2019; 248: 573-586.
50. Hu C, An J. F, Xie Y.F, et al. Mn modified phosphotungstic acid, a highly selective catalyst for the synthesis of 9, 9-bis (4-aminophenyl) fluorene. Applied Catalysis A: General 2021; 626:118358.
51. Li X.Y, Lu X.B, Hu W.X, et al. Phosphotungstic acid functionalized biochar for furfural production from corncob. Fuel Processing Technology 2022; 229:107178.

52. Wang T, Qu S.S, Wang J.H, et al. W/Mo-heteropoly blue-modified defective $W_{18}O_{49}$ as Z-Scheme heterostructure photocatalysts for efficient N_2 fixation. Journal of Alloys and Compounds 2023; 938: 168631.
53. Li J.P, Chen W.L, Chen L, et al. A strategy to obtain long-term stable heteropoly blues for photosensitive property investigations. Advanced Optical Materials 2018; 6: 14.
54. Du L.B, Riu R.W, Sudem B, et al. Development of phosphotungstic acid immobilized amine-grafted graphene oxide as heterogeneous catalyst for synthesis of bis(indolyl)methane derivatives. Polyhedron 2023; 244:116584.

Figures

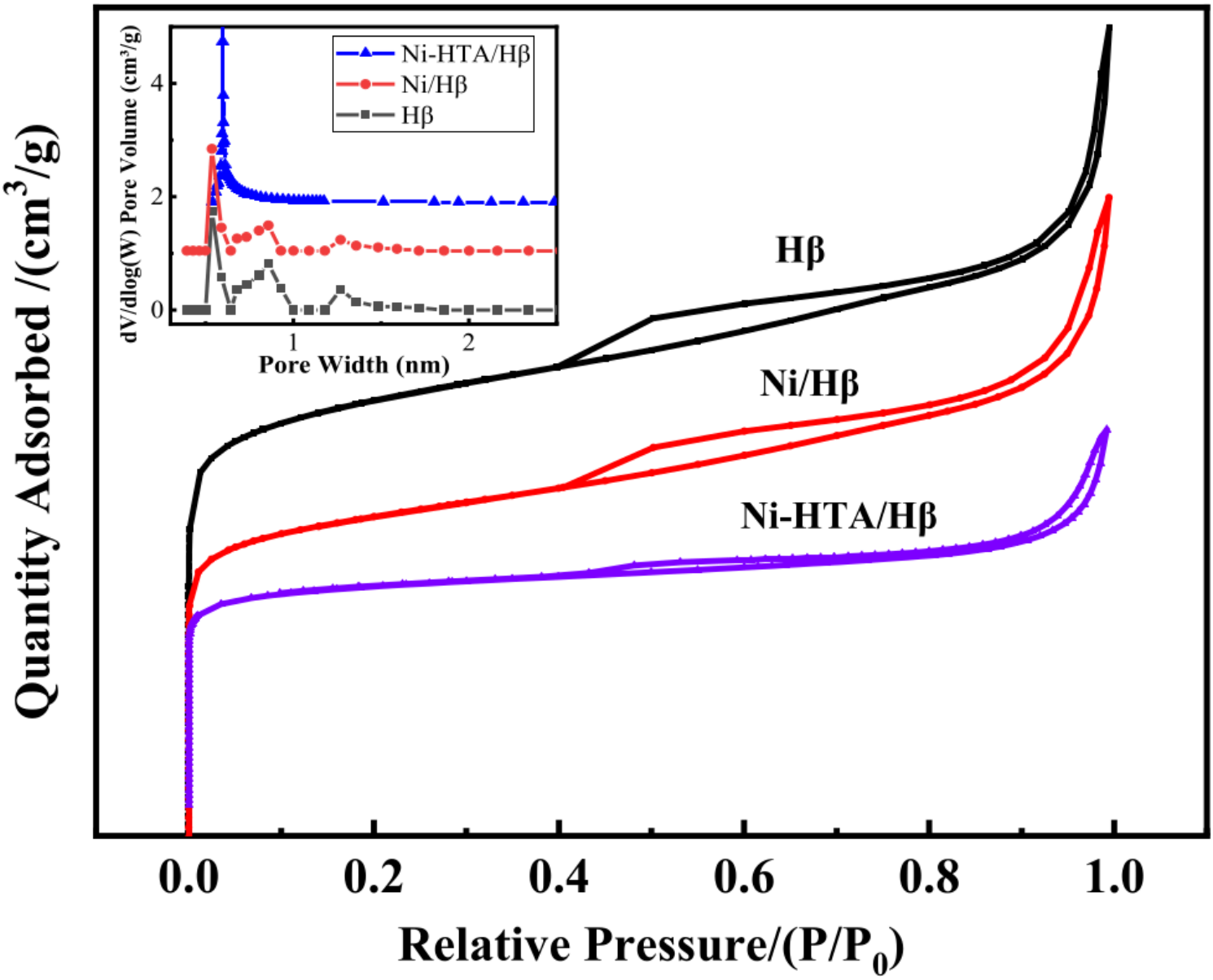

Figure 1

Fig. 2 Nitrogen adsorption and desorption isotherms and pore size distribution

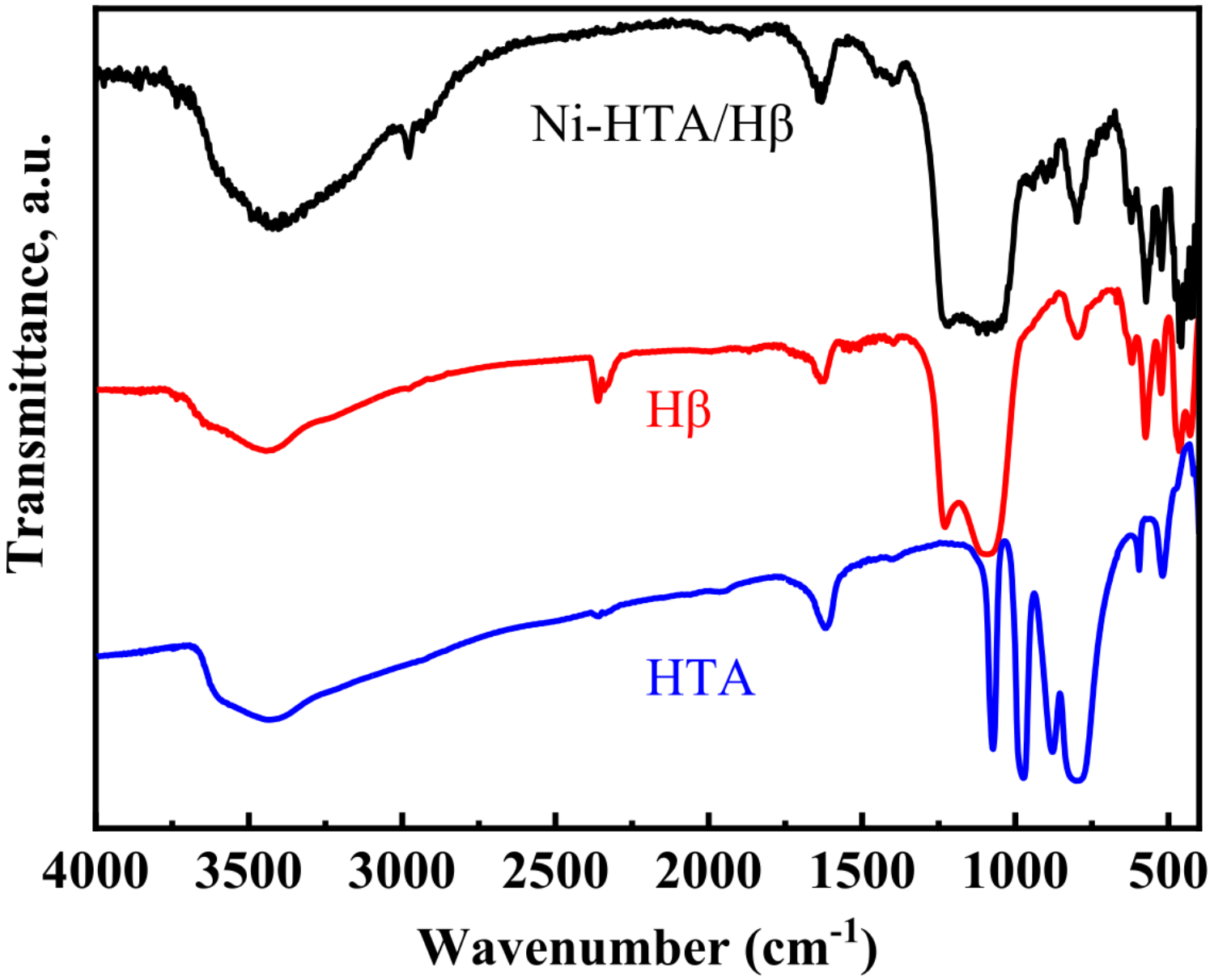

Figure 2

Fig. 3 Infrared spectra of catalyst Ni-HTA/Hβ, Hβ and HTA

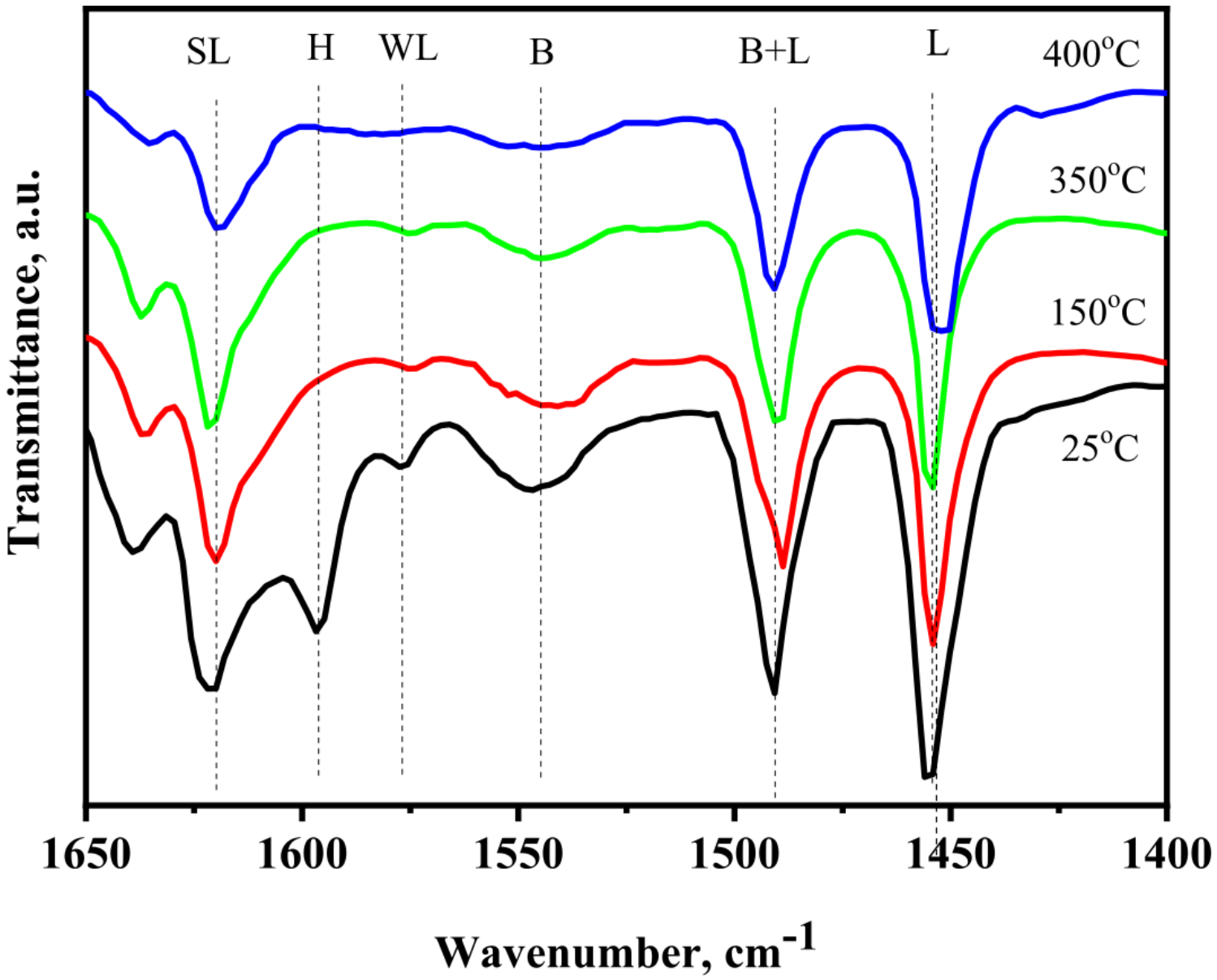

Figure 3

Fig. 4 Pyridine infrared of Ni-HTA/Hβ

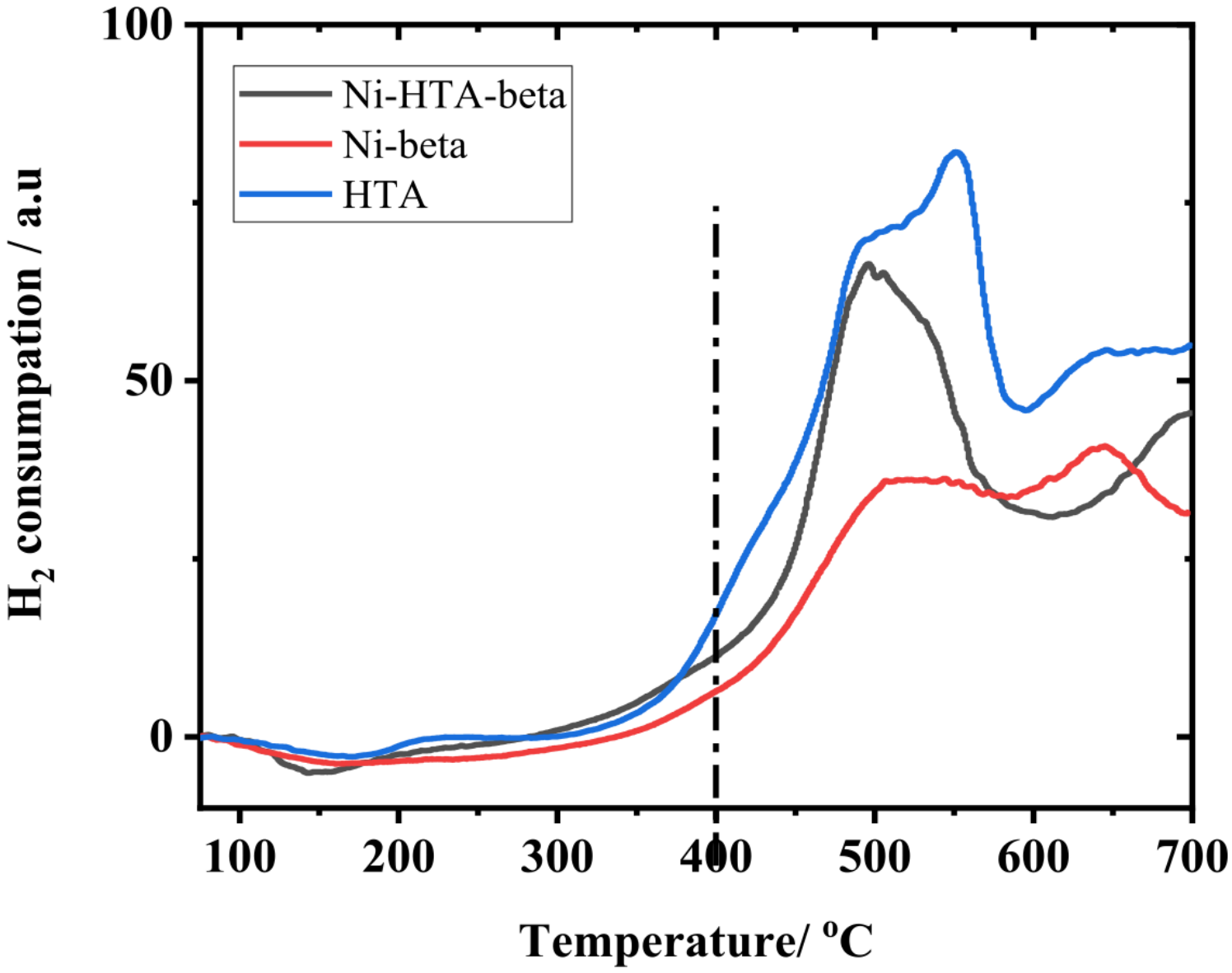

Figure 4

Fig. 5 The H_2-TPR profiles of Ni-HTA/Hβ and HTA

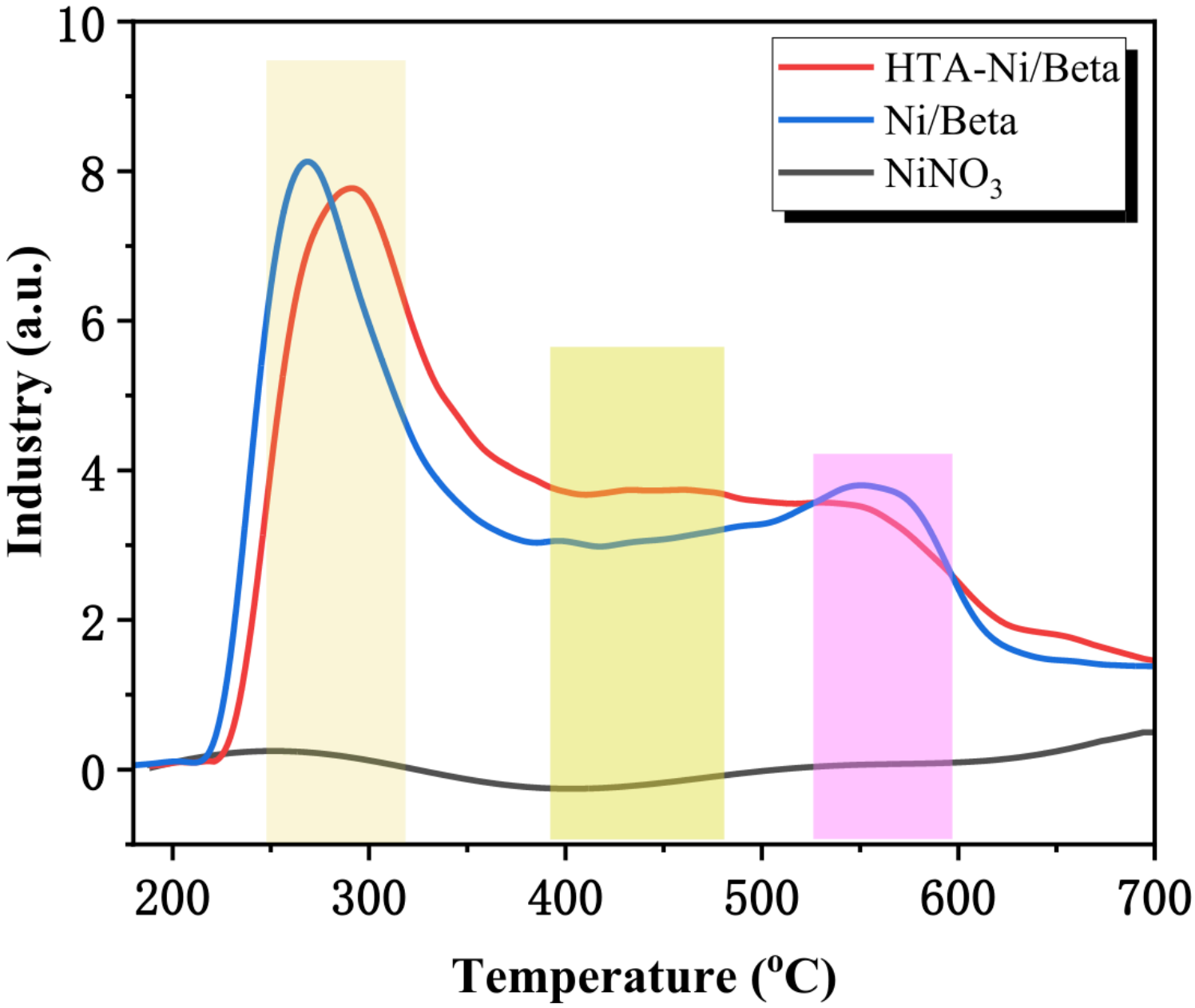

Figure 5

Fig. 6 The result of NH_3-TPD of samples

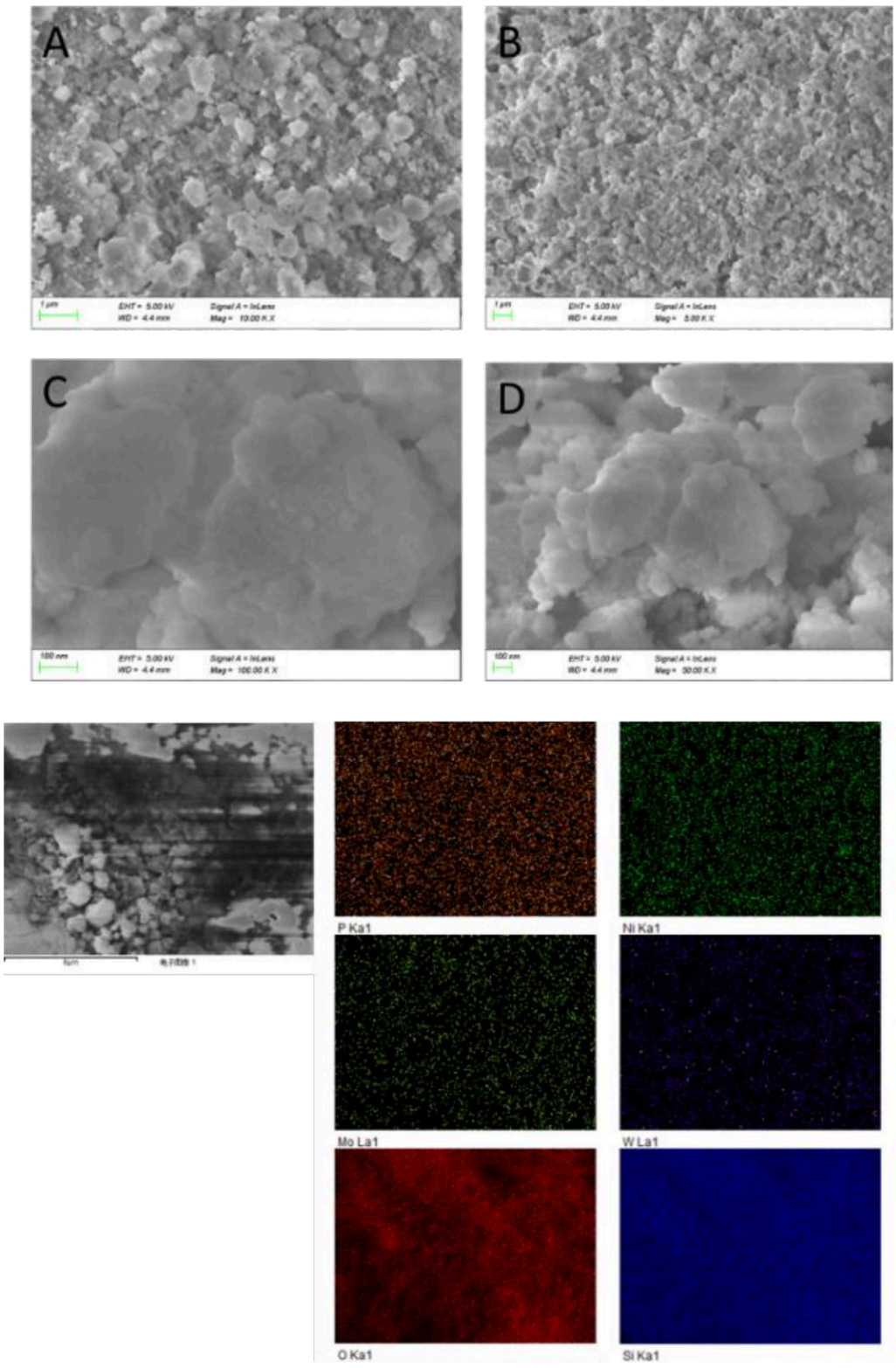

Figure 6

Fig. 7 SEM image and mapping of Ni-HTA/Hβ

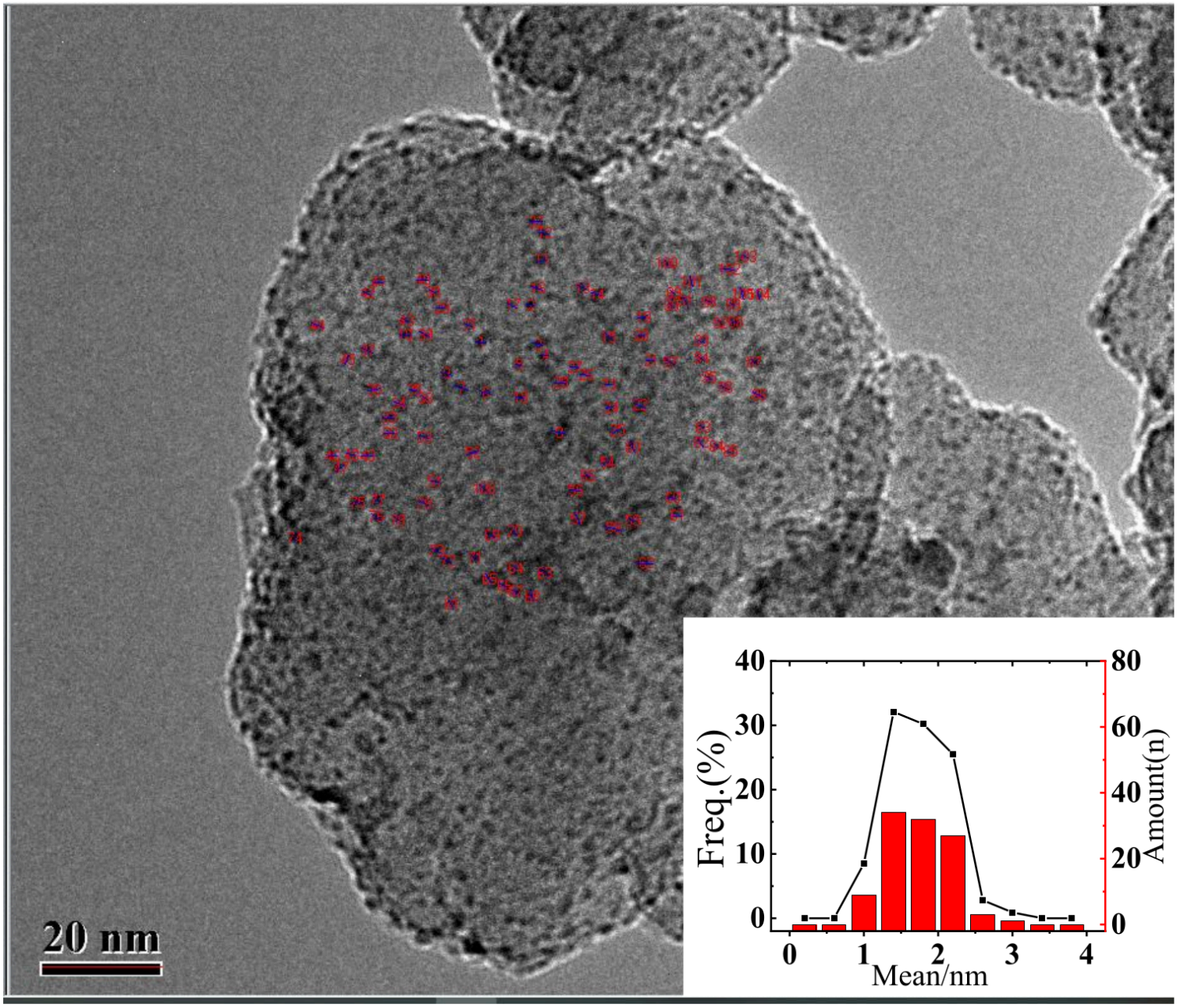

Figure 7

Fig. 8 TEM image of Ni-HTA/Hβ

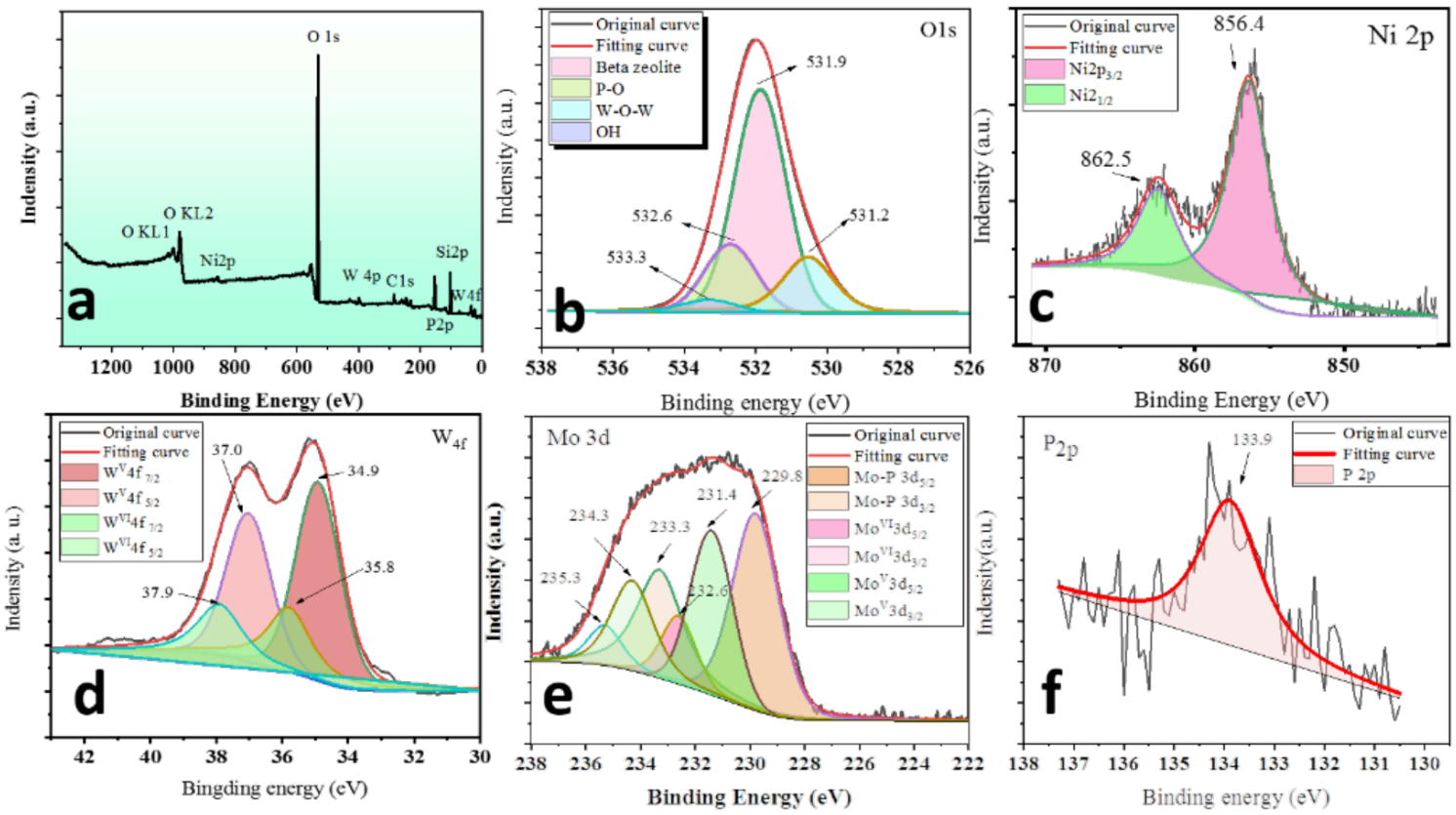

Figure 8

Fig. 9 (a) Complete XPS spectrum and High resolution XPS spectrum of (b) O1s, (c) Ni2p, (d) W 4f, (e) Mo3d and (f) P2p of Ni-HTA/Hβ.

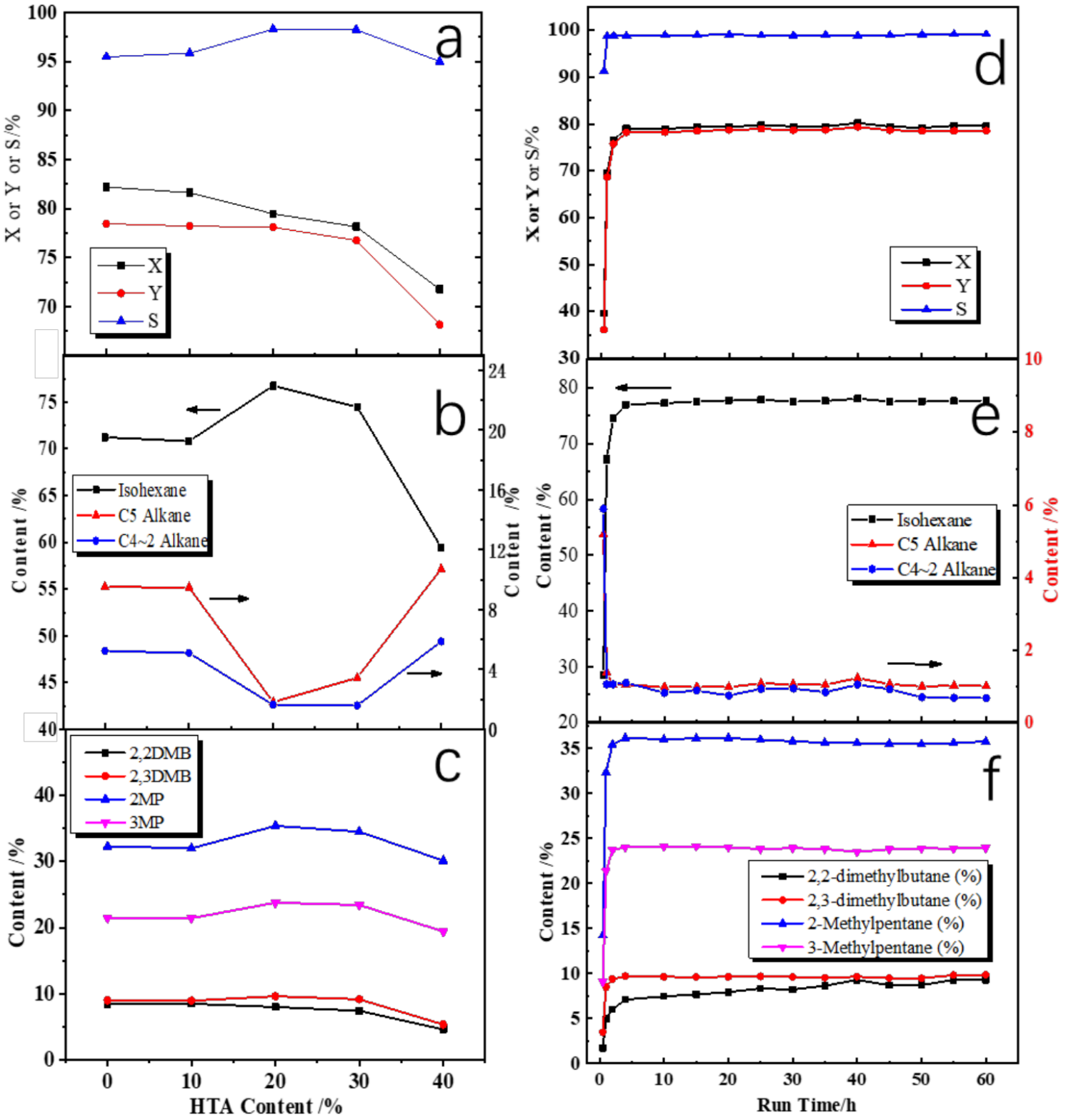

Figure 9

Fig. 10 The effect of the content of HTA on isomerization performance and long term operation of Ni-HTA/Hβ catalyst for n-hexane. The a (d) is the overall catalytic performance, the b (e) and c (f) are the contents of isohexane, C^5 alkane and small molecule alkane, and kinds of C_6 isoalkanes.

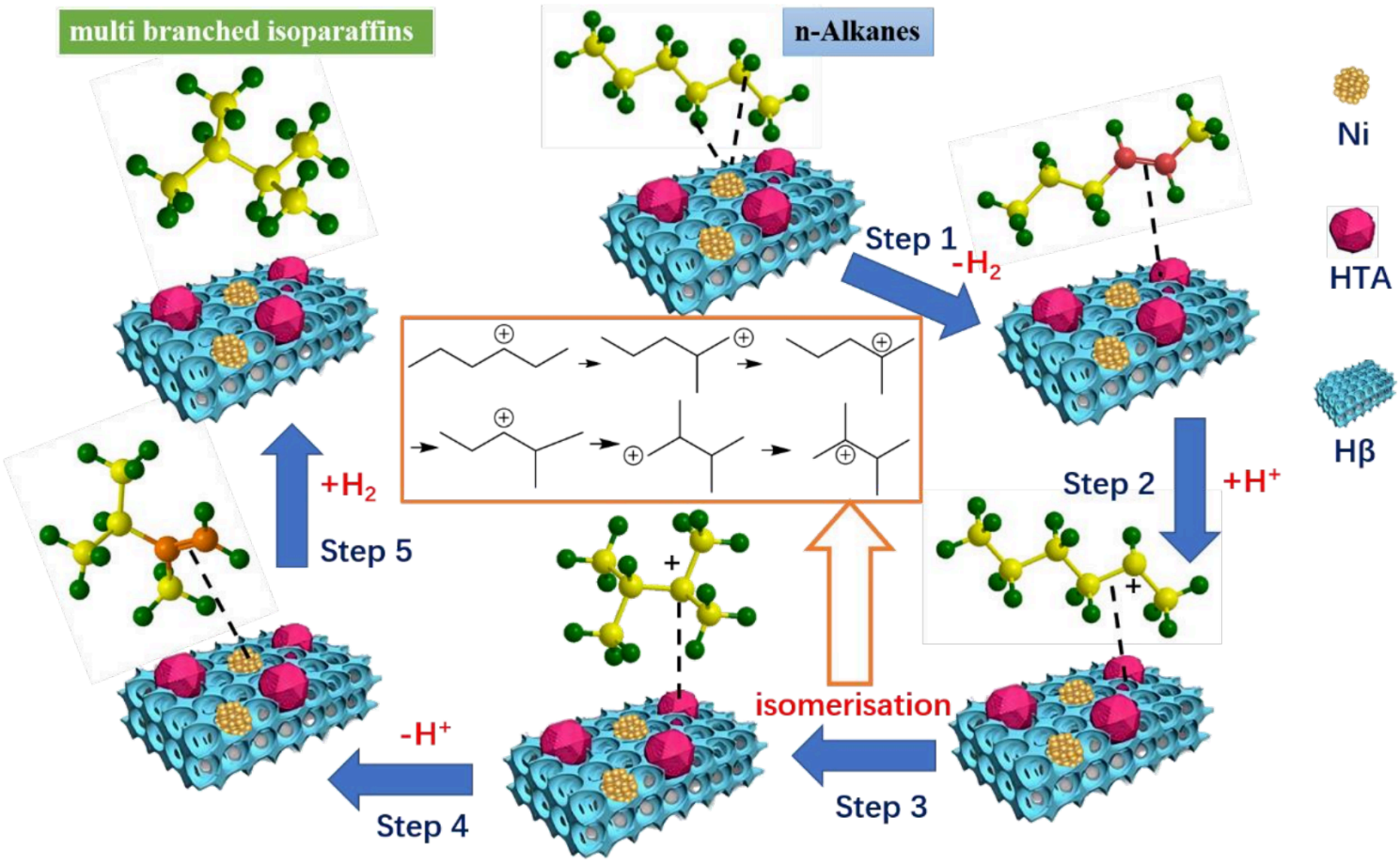

Figure 10

Fig. 11 The reaction mechanism of preparing multi-branched alkanes from n-alkanes on Ni-HTA/H β. The central illustration shows the mechanism of carbocation isomerization reaction.

Supplementary Files

This is a list of supplementary files associated with this preprint. Click to download.

- SupplementaryMaterial.docx
- floatimage1.png